

# Development of Niobium Nitride Thin Film for Next-Generation Superconducting Acceleration Cavities

Ryohei ITO<sup>\*1</sup> and Tomohiro NAGATA<sup>\*1</sup>

<sup>\*1</sup>Future Technology Research Laboratory, ULVAC, Inc., 516 Yokota, Sannu, Chiba, 289-1226, Japan

S-I-S (superconductor-insulator-superconductor) multilayered structure theory has been proposed to achieve the maximum acceleration gradient of superconducting radio frequency cavities higher than the theoretical limit of conventional Nb cavities. In order to demonstrate this theory, we investigated the optimal deposition condition for reactive sputtering of NbN-SiO<sub>2</sub> thin films and the correlation between the deposition conditions and the thin film properties. We finally made a multilayered sample consisting of NbN-SiO<sub>2</sub> thin films and bulk Nb substrate, which has good crystalline orientation. Moreover, we clarified that the lower critical field of the multilayered sample was higher than a bulk Nb. In other words, we succeeded in demonstrating the S-I-S theory for the first time using a small sample size for measurement purposes.

## 1. Introduction

When a strong RF electrical field is applied to a superconducting acceleration cavity in order to accelerate charged particles, a strong magnetic field is also generated simultaneously on the inner wall surface of the cavity. The maximum acceleration gradient ( $E_{acc}$ ) of the charged particles is proportional to the strength of the magnetic field that can be applied to the cavity. Because Nb, which is used as a superconducting acceleration cavity material, is a Type-II superconductor, it can maintain a quasi-stable superconducting state, even when the strength of the magnetic field exceeds the lower critical field value ( $H_{cl}$ ). In terms of a specific value, the lower critical field value is approximately 180 mT in the case of ideal Nb<sup>1)</sup>. However, if an even stronger magnetic field is applied that exceeds the threshold value, heating on the inner wall surface of the cavity ends up destroying the superconducting state. This is called a quench. In order to raise the point at which the Nb cavity reaches a quench, i.e., the maximum acceleration gradient ( $E_{acc}$ ), technologies for manufacturing cavities have been the subject of continuous research for many years. At present,  $E_{acc}$  is already approaching the theoretically implied limit and no further significant improvements can be expected<sup>1), 2)</sup>. Note that theoretically the specific maximum value for the magnetic field that can be withstood is approximately 200 mT<sup>1)</sup>.

For this reason, a theory has been proposed in recent years that the magnetic field applied to the Nb can be weakened by creating a superconductor-insulator-superconductor (S-I-S) multilayered structure, by means of forming a superconductor layer and an insulator layer on the inner wall surface of the cavity (Figure 1)<sup>3)-5)</sup>. According to this theory, if appropriate thicknesses are selected for the superconducting and insulator layers, the effective  $H_{cl}$  of the cavity supposedly improves, making it possible to achieve a level of  $E_{acc}$  that has not been attainable in conventional Nb cavities. Theoretically, at least NbN and Nb<sub>3</sub>Sn are shown to be effective as superconductive layers, and computation results have been obtained showing that maxima of around 240 mT and 400 mT can be achieved using NbN and Nb<sub>3</sub>Sn, respectively<sup>5)</sup>. However, because the physical properties of

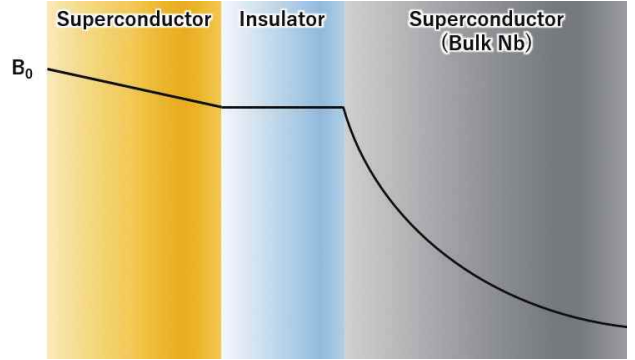


Figure 1 Magnetic field attenuation example in the multilayered structure.

the superconductive layer used in this theoretical computation assume values possessed by a bulk superconductive material, an actually fabricated thin film may not necessarily show results matching the theory. Therefore, validation of the theory and technology for manufacturing a high-quality S-I-S multilayered structure are needed. Our motivation is to establish basic principles for next-generation superconducting acceleration cavities and a technology for their manufacture.

What is important from the viewpoint of theoretical verification is to establish a measurement system that can be used for simple evaluation using a small sample size, as well as a technology that can be used to manufacture samples relatively simply and with excellent replicability. The value of  $E_{acc}$  cannot be measured unless a cavity is actually manufactured, which would require massive amounts of expense and time, as well as a technology for depositing a film uniformly on the interior surface of a cavity that has a complex shape<sup>6)</sup>. However, for purposes of comparison with conventional Nb, measuring the aforementioned effective  $H_{cl}$  on a small number of samples would be sufficient<sup>7)</sup>. For measuring  $H_{cl}$  on a small number of multilayered thin-film samples, a practical example using the third-harmonic measurement method has already been reported<sup>8)</sup>. Note, however, that this practical example uses thin-film Nb as the superconductive layer, which is the substrate for the S-I-S multilayered structure. It is presumed that  $H_{cl}$  exceeding that of bulk Nb is not possible to achieve, even if an S-I multilayered film were deposited on the surface, because the  $H_{cl}$  value of thin-film Nb is extremely small. For manufacturing multilayered

<sup>\*1</sup> Future Technology Research Laboratory, ULVAC, Inc., 516 Yokota, Sannu, Chiba, 289-1226 Japan.

Table 1 Sputtering conditions for NbN and SiO<sub>2</sub> thin films.

Thin film material	Condition name	Input power [kW]	Ar gas flow rate [Pa · m <sup>3</sup> /s]
NbN	A	DC 3.0	0.186
	B	DC 6.0	0.186
	C	DC 6.0	0.383
	D	DC 6.0	0.862
SiO <sub>2</sub>	E	AC 6.0	0.186

thin-film samples to be used for measuring  $H_{c1}$ , sputtering is appropriate. The reasons are as follows: first, it is considered that an NbN thin film with excellent crystallinity and uniform composition can be obtained relatively easily using reactive sputtering. Additionally, it is easy to guarantee replicability by controlling such conditions as the gas pressure for film deposition. Note that the theory does not refer specifically to the physical properties of the insulating layer, so the type of material to be selected is unknown. However, in this example, we selected SiO<sub>2</sub> because it can be obtained easily using reactive sputtering.

In this article, we will describe deposition examples of NbN thin film and SiO<sub>2</sub> thin film, and provide evaluation results of each individual layer, manufacturing examples of S-IS multilayered structure samples, and  $H_{c1}$  measurement results.

## 2. Film deposition system and method

The samples to be used for measuring  $H_{c1}$  using the third-harmonic measurement method must possess uniform film thickness. If the actual film thickness differs from the film thickness assumed for the measurement location, the reliability of the measurement result will be destroyed. The effects of such a difference in film thickness are especially noticeable in the case of superconductive layers. For this reason, we ensured film thickness uniformity in the substrate transfer direction by using an interback film deposition system. In addition, for the direction perpendicular to the transfer direction, we checked replicability by performing a film thickness measurement test multiple times beforehand. Measurements using a contact-type step gauge showed that the NbN film thickness was 200 nm,  $\pm 10$  nm. Therefore, measurement errors stemming from the NbN film thickness at  $H_{c1}$  in this NbN film thickness region are expected to be at the most plus or minus just a few mT at a temperature of 2 K. Changes in the SiO<sub>2</sub> film thickness will have an even more minute effect than changes in the NbN film thickness. Measurements using a spectroscopic ellipsometer showed that the SiO<sub>2</sub> film thickness was 30 nm,  $\pm 1$  nm. From here on, the NbN film thickness will be assumed to be 200 nm and the SiO<sub>2</sub> film thickness, 30 nm, unless indicated otherwise.

Both NbN and SiO<sub>2</sub> films were deposited using reactive sputtering. For depositing the NbN film, a gas mixture of Ar and N<sub>2</sub> was introduced into the sputtering chamber, and a DC voltage was applied to an Nb cathode to cause an electrical discharge. For depositing the SiO<sub>2</sub> film, a gas mixture

of Ar and O<sub>2</sub> was introduced into the sputtering chamber, and an AC voltage was applied to two Si cathodes. In both cases, a constant power supply was controlled to ensure that a preset voltage would be applied. If the N<sub>2</sub> or O<sub>2</sub> gas flow rate is varied while the Ar flow rate is kept constant, the discharge voltage or current will vary in response. Naturally, the film composition will also vary at the same time. Using this relationship, we searched for and determined the appropriate N<sub>2</sub> or O<sub>2</sub> gas flow rate that corresponds to the power that was set. Table 1 shows the DC or AC power that was set at a constant value, as well as the Ar gas flow rate used in this example.

## 3. NbN film deposition and evaluation

### 3.1 Search for the ideal film deposition conditions

As an index for expressing the characteristic of superconductive materials, the superconducting critical temperature ( $T_c$ ) is well known. In other words,  $T_c$  is the temperature at which  $H_{c1}$  begins to climb; if a material is to be used for the acceleration cavity, the higher the  $T_c$ , the better. Figure 2 shows an example of the temperature characteristic of  $H_{c1}$  assuming an ideal Nb bulk. In this case,  $T_c$  is 9.2 K, and  $H_{c1}$  begins to rise at this temperature. In the case of a bulk superconductor,  $T_c$  will vary slightly depending on its manufacturing method, but a value derived from a theoretical computation can generally be obtained, provided that the composition ratio is appropriate and uniform. However, in the case of a thin-film superconductor, distortion in the crystal lattice resulting from the thin-film growth process might cause  $T_c$  to deteriorate even when the composition ratio is uniform. Therefore, when handling a thin-film superconductor, it is necessary to determine the optimum film deposition conditions by depositing the film so that the appropriate composition ratio is achieved under a variety of film deposition conditions, and further, by measuring  $T_c$  of the obtained thin films one by one.

Note that high-accuracy measurement of  $T_c$  requires technology and time. This is because it is crucial to slowly cool the sample to a temperature lower than  $T_c$  while maintaining temperature stability, or to slowly warm the sample from a temperature lower than  $T_c$  while maintaining temperature stability. Such a method is not very suitable for fabricating a large number of thin-film samples and evaluating them one by one. Therefore, as the first step, we evaluated crystal orientation by measuring at room temperature the resistivity and XRD of Nb<sub>1-x</sub>N<sub>x</sub> thin film deposited while varying the N<sub>2</sub>

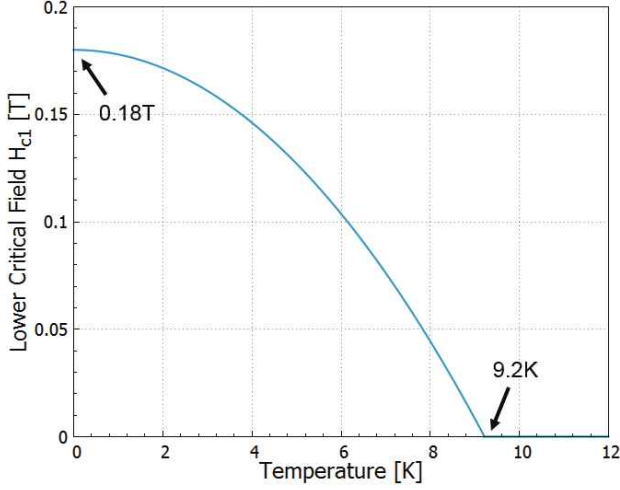


Figure 2 Ideal  $H_{cl}$  curve of bulk Nb.

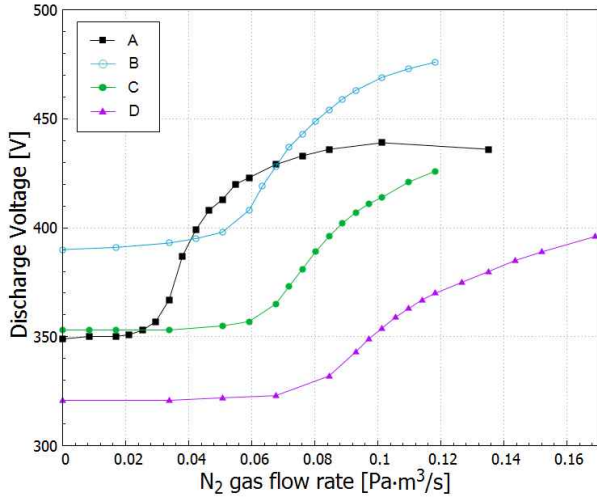


Figure 3 Discharge voltage for varying  $N_2$  gas flow rates.

flow rate under the various film deposition conditions listed in Table 1. Afterwards, we selected the best condition for each film deposition parameter, and then measured  $T_c$  of the thin films deposited under those conditions.

Figure 3 shows the changes in the discharge voltage when the  $N_2$  gas flow rate is varied under the various film deposition conditions. Next, Figure 4 shows the changes in the resistivity of the  $Nb_{1-x}N_x$  thin film when the  $N_2$  gas flow rate is varied under the various film deposition conditions. In the case of reactive sputtering of an NbN film, the discharge voltage increased monotonously as the  $N_2$  gas flow rate increased. We were also able to confirm that an  $N_2$  flow rate region exists where the discharge voltage increases substantially. Before and after this  $N_2$  flow rate region, the composition of the  $Nb_{1-x}N_x$  thin film can be considered to have changed significantly. In these same regions, the resistivity also exhibits peculiar changes such that there is a minimum value in each region. However, as the gas pressure increases, the resistivity's tendency to decline temporarily weakens, and no peculiar minimum value is seen under condition (D), i.e., input power of 6 kW and Ar gas flow rate of  $0.862 \text{ Pa} \cdot \text{m}^3/\text{s}$ .

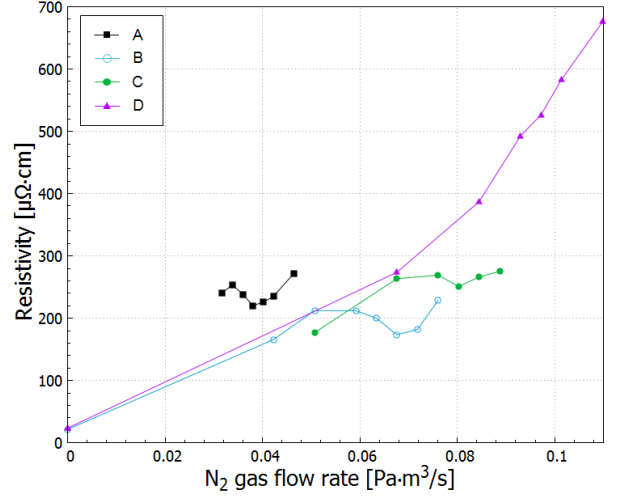


Figure 4  $Nb_{1-x}N_x$  thin film resistivity at room temperature for varying  $N_2$  gas flow rates.

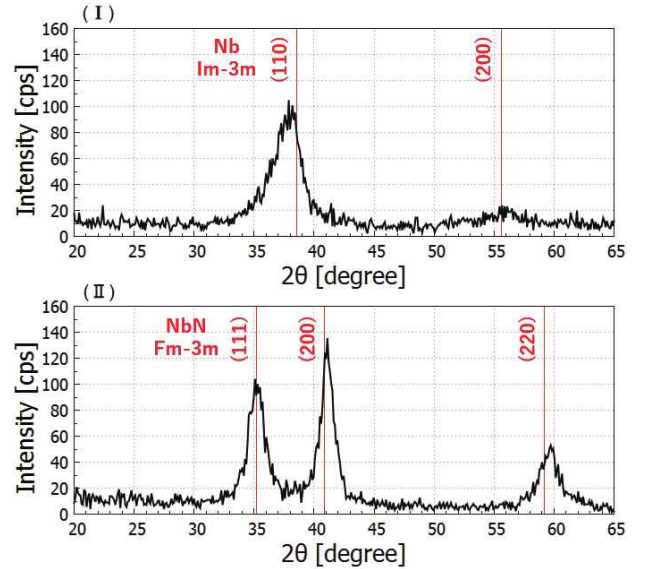


Figure 5 XRD patterns of NbN-glass samples measured by the in-plane method.

Superconducting NbN is known to have an NaCl type (Fm-3m) crystal structure with a composition ratio of 1:1 in terms of atomic ratio. Figure 5 shows the XRD measurement results of an  $Nb_{1-x}N_x$  thin film deposited on a glass substrate under condition (B), i.e., input power of 6 kW and Ar gas flow rate of  $0.186 \text{ Pa} \cdot \text{m}^3/\text{s}$ . In the  $N_2$  flow rate region (I) before the discharge voltage increases significantly, the peak does not match NbN (Fm-3m). Instead, this peak is closer to Nb (Im-3m), and it can be seen that the volume of N is still small in this region. While the discharge voltage is increasing significantly, that is, in the  $N_2$  gas flow rate region (II) near where the resistivity has a minimum value, the peak closely matches NbN (Fm-3m). In other words, the composition ratio of the film can be considered to be approximately 1:1. In the  $N_2$  gas flow rate region after the discharge voltage has finished increasing significantly, there is too much N inside the film. Consequently, the inter-lattice distance increases, shifting the peak position to the lower-angle side.

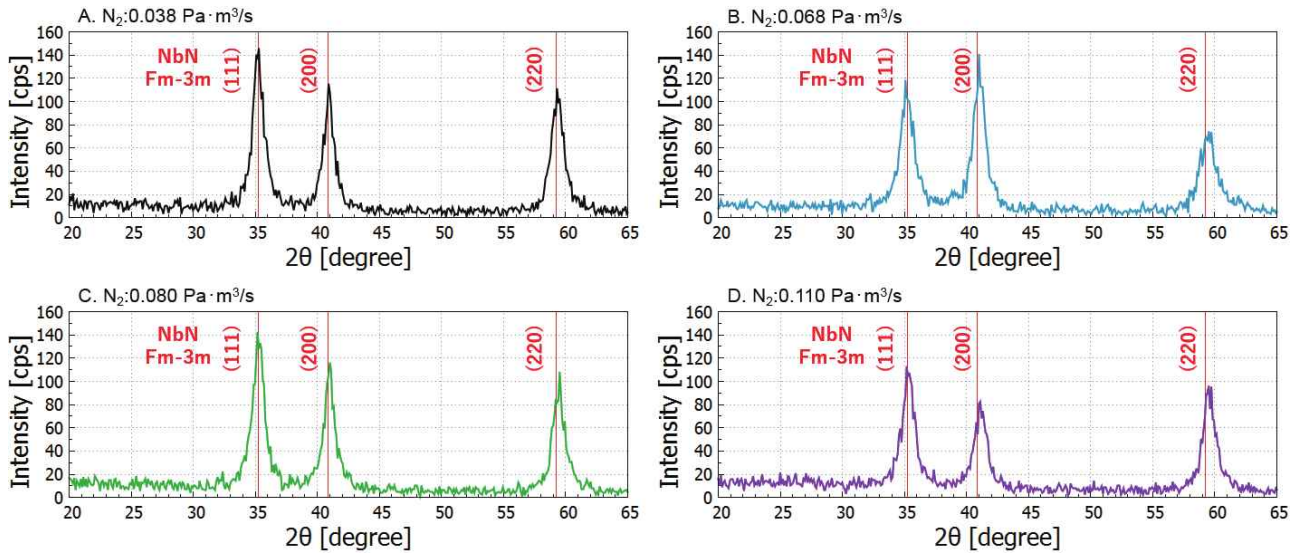


Figure 6 XRD patterns of NbN-Si samples measured by the in-plane method.

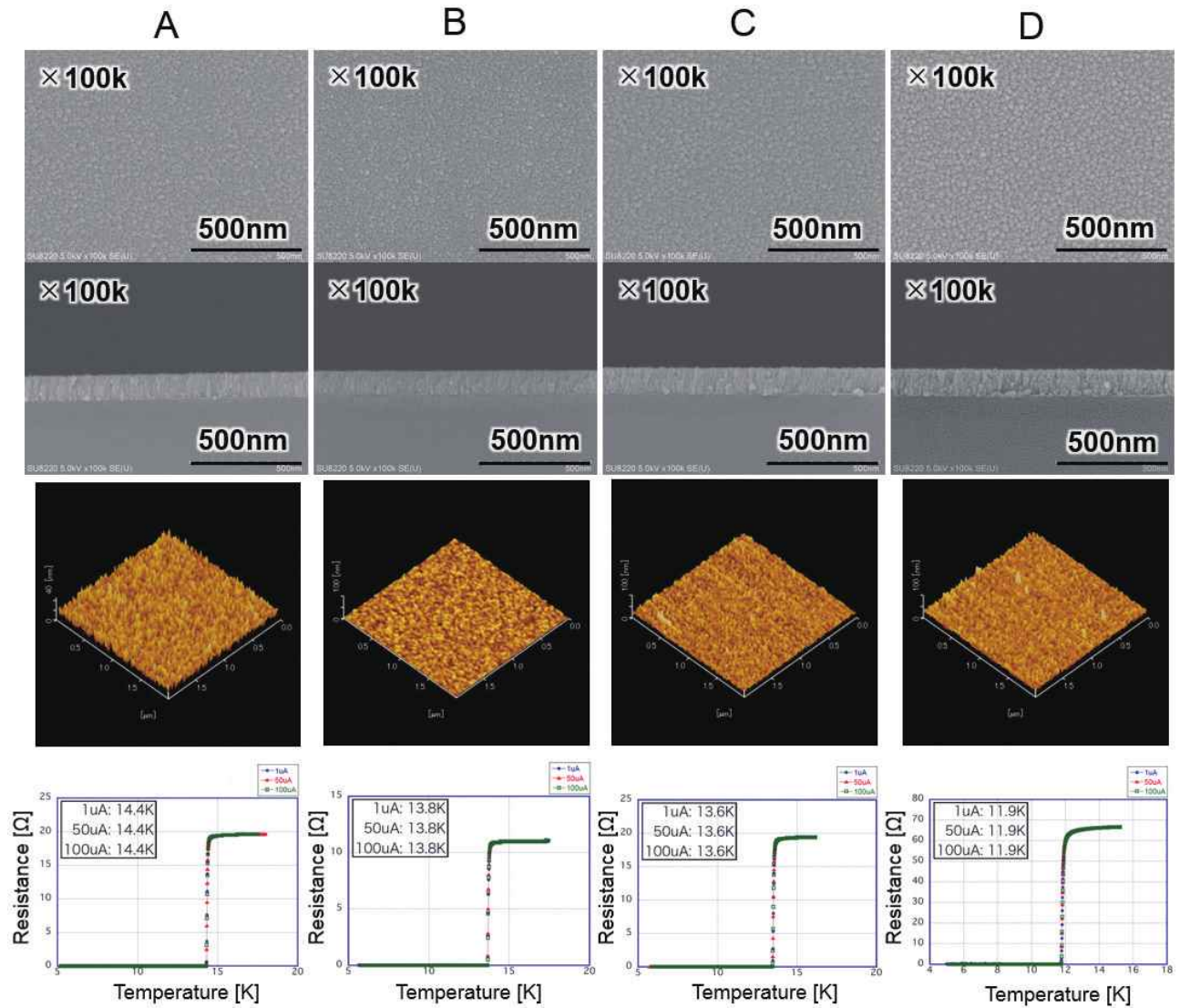


Figure 7 NbN thin film properties.

Therefore, by looking at the changes in the discharge voltage and resistivity, it is possible to determine the crystal-

linity and approximate composition ratio of the  $\text{Nb}_{1-x}\text{N}_x$  thin film, even without making XRD measurements.

Table 2 Surface roughness, film density, film stress and  $T_c$ .

	Surface roughness [nm]	Film density [g/cm <sup>3</sup> ]	Film stress [MPa]	$T_c$ [K]
A	3.34	7.84	-492	14.4
B	1.37	8.38	-975	13.8
C	3.11	7.12	- 78	13.6
D	3.37	6.15	-115	11.9

Similar trends were also confirmed in the power input and Ar gas flow rate conditions. Figure 6 summarizes samples in which the XRD peak best matched NbN (Fm-3m) under various film deposition conditions. All of these sample films were deposited on Si wafers.

### 3.2 Investigation of NbN thin film properties

As mentioned above, computations made in the theory for S-IS multilayered structures assume the physical properties of the NbN layer to be the same as those of a bulk material. Therefore, we wanted to assess how far the physical properties of an actual NbN thin film differ from those of a bulk material. To do so, we evaluated SEM, AFM, film density, film stress, and  $T_c$ , using samples in which films were deposited on Si wafers under the four types of conditions A through D shown in Figure 6.  $T_c$  was measured using the four-terminal method. Although three different current values were input, the results did not change significantly from case to case. Figure 7 and Table 2 summarize the evaluation results. All the NbN films obtained had a columnar structure and, on Si, were basically highly dense films with little surface roughness. This tendency was strong under conditions of especially low or especially high power, but, on the other hand, these films exhibit extremely large compressive stress. The measurement result of  $T_c$  was the highest, at 14.4 K, under condition (A), i.e., input power of 3 kW and Ar gas flow rate of 0.186 Pa · m<sup>3</sup>/s. In other words, an excellent value close to the  $T_c$  of bulk NbN (16 K) was obtained, even on a thin film. These  $T_c$  values are considered to have resulted from the compound effect produced by various factors, such as the crystallinity of the thin film and the distortion caused by stress. To understand a more detailed correlation, more data needs to be accumulated.

## 4. SiO<sub>2</sub> film deposition and evaluation

The SiO<sub>2</sub> film was deposited using the same equipment used for the NbN film. This is because we attached importance to the fact that two layers can be deposited continuously without exposing them to the atmosphere when fabricating the S-IS multilayered structure samples. In this example, under the conditions of constant input power and the same Ar gas flow rate as was used with the NbN film, only the O<sub>2</sub> gas flow rate was varied and the resulting discharge voltage characteristics were observed. Figure 8 shows the changes in the discharge voltage in response to changes in the O<sub>2</sub> gas flow rate. In the case of SiO<sub>2</sub>, an O<sub>2</sub> gas flow rate region exists where the discharge voltage drops

Table 3 Refractive index of SiO<sub>2</sub>.

Measurement sample	Film thickness [nm]	Refractive index @633nm
Sputtered film	96.1	1.47844
Thermal oxide film	103.3	1.46464

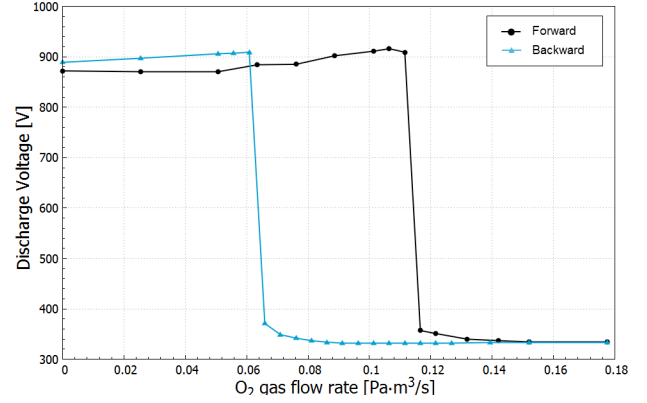


Figure 8 Discharge voltage for varying O<sub>2</sub> gas flow rate.

substantially and, in addition, the characteristic of hysteresis is evident. Because we knew from our experience that SiO<sub>2</sub> thin film can be obtained in a region that is slightly past this flow rate region and in which the discharge voltage has stabilized, we set the O<sub>2</sub> gas flow rate to 0.152 Pa · m<sup>3</sup>/s.

When we used a spectroscopic ellipsometer to measure the refractive index of a film that had been deposited on an Si wafer to a thickness of around 100 nm, we were able to obtain a value close to the refractive index of an Si oxide film (100 nm) used for comparison purposes. Table 3 shows the results.

## 5. Fabrication and evaluation of H<sub>c1</sub> samples

We will now describe an example in which we fabricated an S-IS multilayered structure based on the NbN and SiO<sub>2</sub> film deposition conditions described in Sections 3 and 4. For the NbN film deposition conditions, we adopted input power of 3 kW and an Ar gas flow rate of 0.186 Pa · m<sup>3</sup>/s, which had produced the highest  $T_c$ . For the substrate, we used an Nb plate 2.8 mm in thickness cut to 48 mm × 58 mm. Before film deposition, we applied three surface treatments to the substrate: electro polishing (EP), vacuum annealing, and EP again.

Figure 9 shows the external appearance of the Nb plate sample before and after deposition of the NbN-SiO<sub>2</sub> film. While the Nb substrate before film deposition (left) appears silvery white, the substrate appears blackish golden after the NbN-SiO<sub>2</sub> film was deposited (right). It can be seen that the same mirror surface is present before and after film deposition, indicating that the surface roughness did not change much. Figure 10 shows the XRD pattern measured after the deposition of the NbN-SiO<sub>2</sub> film. We could confirm only the Nb (Im-3m) and NbN (Fm-3m) peaks of the substrate. The



Figure 9 Nb substrates before and after coating.

peak intensity ratio of NbN hardly fluctuated regardless of the measurement location, and an NbN film with (111) as the main orientation had been uniformly deposited. Note that because the peak in Nb indicates the crystal orientation of the bulk substrate, the intensity ratio varies depending on the measurement location.

Furthermore, using this S-I-S multilayered structure sample, we measured  $H_{cl}$  based on the third harmonic. Detailed results were reported by our joint research group at the 9th International Particle Accelerator Conference (IPAC '18)<sup>9)</sup>. To summarize the content of this report, the NbN-SiO<sub>2</sub>-Nb multilayered structure sample exhibited a higher  $H_{cl}$  than an Nb sample that received similar surface treatments but no film deposition. This is the first example in which the theory concerning S-I-S multilayered structures was proven based on measurements from a small sample size. When  $H_{cl}$  at 2 K is estimated from an approximation curve drawn using actual data from an S-I-S multilayered structure sample, it is between 220 and 230 mT, roughly matching the value computed from the theory<sup>9)</sup>. However, so far, we have only been able to obtain data points near 9.2 K, which is the  $T_c$  of Nb. Therefore, it must be noted that the errors in the approximation curve may be large. To draw an accurate approximation curve, it will be necessary to acquire data on the lower-temperature side and the higher magnetic field side. Furthermore, if we can increase the number of data points in the region near 9.2 K to 14 K, the approximation accuracy of the  $H_{cl}$  curve, generated by the effect of the NbN thin film only, can also be expected to improve.

## 6. Conclusion

This article discussed deposition of NbN and SiO<sub>2</sub> thin films toward achieving next-generation superconducting cavities (establishment of a theory on S-I-S multilayered structures), fabrication of S-I-S multilayered structure samples using these thin films, and measurement of  $H_{cl}$ . Ultimately, we succeeded for the first time anywhere in fabricating an NbN-SiO<sub>2</sub>-Nb sample with a higher  $H_{cl}$  than that of bulk Nb, and we demonstrated the feasibility of S-I-S multilayered structures.

Our primary goal for future work is to improve the reliability of the approximation curve for  $H_{cl}$ . We are also planning to conduct supplementary tests using different measuring

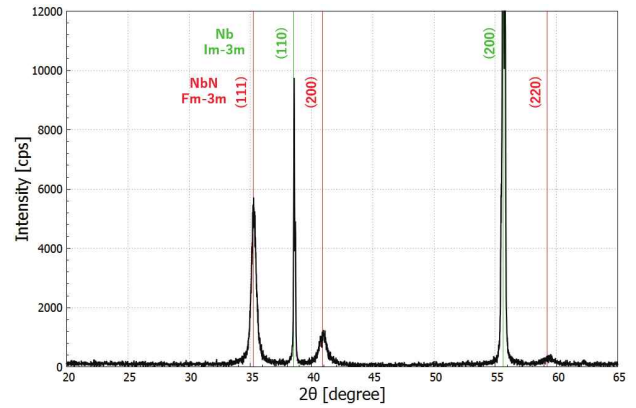


Figure 10 XRD pattern of NbN-SiO<sub>2</sub>-Nb sample measured by the out-of-plane method.

equipment. We also plan to measure  $H_{cl}$  when a magnetic field is applied in a frequency band close to that of an actual acceleration cavity. If the evaluation of high-frequency magnetic field radiation in these supplementary tests proves the validity of the theoretical computation for an S-I-S multilayered structure, an S-I-S multilayered structure utilizing Nb<sub>3</sub>Sn should make it possible to achieve  $H_{cl}$  of 400 mT or higher, which has not previously been possible. In reality, several major issues remain, such as the need to develop a technique for depositing a film on the inner wall surface of the cavity. Nevertheless, our research toward realizing a next-generation superconducting cavity is progressing well for the time being.

Note that this article incorporates corrections to and revisions of “Development of Coating Technique for Superconducting Multilayered Structure,” which was part of the Proceedings reported at the 9th International Particle Accelerator Conference (IPAC '18).

## References

- 1) W. Singer, S. Aderhold, A. Ermakov, J. Iversen, D. Kostin, G. Kreps, A. Matheisen, et al.: Phys. Rev. ST Accel. Beams **16** (2013) 012003.
- 2) H. Padamsee, J. Knobloch and T. Hays: *RF Superconductivity for Accelerators* (John Wiley, New York, 1998) p. 71–81.
- 3) A. Gurevich: Appl. Phys. Lett. **88** (2006) 012511.
- 4) A. Gurevich: Rev. Accel. Sci. Technol. **5** (2012) 119.
- 5) T. Kubo, Y. Iwashita and T. Saeki: Appl. Phys. Lett. **104** (2014) 032603.
- 6) Toshio Shishido, et al.: *Performance evaluation of superconducting cavities* (literature distributed at OHO '14), (2014).
- 7) G. Lamura, M. Aurino, A. Andreone and J.-C. Villégier: J. Appl. Phys. **106** (2009) 053903.
- 8) M. Aburas, C.Z. Antoine and A. Four: Proceedings of SRF 2017 (Lanzhou, China).
- 9) R. Katayama, Y. Iwashita, H. Tongu, A. Four, C.Z. Antoine, H. Hayano, T. Kubo, T. Saeki, H. Ito, R. Ito, T. Nagata and H. Oikawa: Proceedings of IPAC 2018, (Vancouver, Canada).